$LiNbO_3$ CHANNEL WAVEGUIDE MODE ANNIHILATION SWITCHING ARRAY AND ITS APPLICATIONS

Ray T. Chen
Physical Optics Corporation
20600 Gramercy Place
Torrance, Ca 90501

ABSTRACT

Optical signal processing and computing require spatial as well as temporal dimensionality. We report thermally annealed cutoff modulator and modulator array that can provide wide modulation bandwidth and multi-channel optical signal processing capability. Experimental results for single channel device and modulator array are presented. A detailed theory is given to explain the theory and the working principle of cutoff modulator. The increase of linear dynamic range of the device after appropriate heat treatment is quantitatively explained. The improvement is due to the proper combination of the coupling condition and the heat-treatment perturbed, electric field induced attenuation coefficient. Modulator array with 333 channels/cm packing density and 1.6 GHz modulation bandwidth is also demonstrated experimentally. Further applications by utilizing the cutoff modulator array, such as addition and subtraction of two numbers and optical logic gate operations are realized also.

2. INTRODUCTION

Electro-optically induced channel guiding and extinction modulation of a light beam in $LiNbO_3$[1-3], $KNbO_3$[4], and GaAs[5-7], were reported recently. Earlier, we described the first reported electro-optic mode annihilation modulator that utilizes a thermally annealed single-mode proton-exchanged channel waveguide in a X-cut, Y-propagating $LiNbO_3$ substrate[3]. The devices we report here can provide not only an easy design and fabrication process but also enhance the integrability of the modulator array due to the simplicity of device structure.

In contrast to the TI devices that are often subject to the photorefractive effect (under zero external electric field) and the concomitant optical damage at a relatively low light intensity, resistance to the optically induced refractive index instability in the PE devices was found to be much larger. For example, no optical damage was observed even after a two hour continuous exposure of the 632.8 nm wavelength He-Ne laser at a light intensity as high as 10^4 W/cm^2. This intensity threshold was at least one order of magnitude higher than that for the Ti-indiffused devices.

In this paper, applications such as multi-channel signal processing and computing, and optical gates are described. An 8-bit parallel optical signal processing and computing device with 333 channels/cm packing density and 1.6 GHz modulation bandwidth is achieved. Binary data flow rate can be introduced to do addition and subtraction operations. Finally, optical gate operations utilizing the exclusive characteristic of the cutoff modulator are delineated.

3. APPLICATIONS OF MODE ANNIHILATION SWITCHING ARRAY

We reported a single-mode electrooptic mode annihilation switch[3] that utilizes a single section of thermally-annealed proton-exchanged (PE) channel waveguide on $LiNbO_3$. The desirable effects of thermal annealing upon the modulator characteristics have been demonstrated including the significant reduction in the drive voltage between minimum transmission (cutoff) and maximum transmission (saturation), the substantial increase in the linearity of modulation, increase of threshold value of optical damage and the enhancement of the stability of the modulator in time domain. In addition, since the modulator requires only a single uniform section of channel waveguide and a corresponding pair of parallel electrodes, simplicity in design and fabrication was also clearly demonstrated. Further applications on this type of device is presented in this section.

3.1 PARALLEL 8-BIT SIGNAL PROCESSING AND COMPUTING DEVICE WITH 3.2 G BIT/SEC CAPABILITY

The new device we have built is on an X-cut, Y-propagating $LiNbO_3$ piece. The masking material is Cr/Al and the exchange solution is pure benzoic acid with 245 ^{o}C and 21 mins exchange time. Three alignment masks needed to fabricate this modulator array are shown in Fig.1. Fig.1.(a) is the lift off mask for channel waveguide formation, Fig.1.(b) the etching mask for electrode pattern and Fig.1.(c) the lay out pattern from the electrodes to bonding pads. The separation between two adjacent channels is 30 microns. The detailed device parameters are listed in Table 1. The measured capacitance including the package is 3.9 pF which gives a 3 db bandwidth of 1.6 GHz. The measured 3db bandwidth through the swept frequency method is given in Fig.2. Frequency response up to 2.0 GHz is also shown in this figure. The results are matched well with the theoretical prediction. The measured cross talk is less than -30db. The measured near field pattern is given in Fig.3. The picture was taken by a Polaroid camera at the image plane with a cylindrical lens as the input coupler and a microscope objective as the imaging lens. The two electrode stripes of each channel of the eight-channel device are separate. A device holder with 16 SMA connectors was made to facilitate the injection of the microwave signals. Two different microwave signals can be applied independently to the two electrode pads associated with each optical channel waveguide.

By utilizing the large linear dynamic range of the thermally annealed mode annihilation modulator array, we can do the mathematical operations such as addition and subtraction with the device electrode configuration shown in Fig.1. Since we employ the linear electrooptic effect to do the operation, the change of the index of refraction as a function of applied voltage can be written as Eq.(1), which gives

$$\Delta N = \frac{-N^3 \cdot r_{33} \cdot E}{2} \qquad (1)$$

where r_{33} is the affiliated electrooptic coefficient and E is the applied electric field which is a vector. The variation of the direction of the electric field will introduce different effects on the index of refraction. One direction will increase the value while the other direction will decrease it. From Eq.(1), it is clear that

(a)

(b)

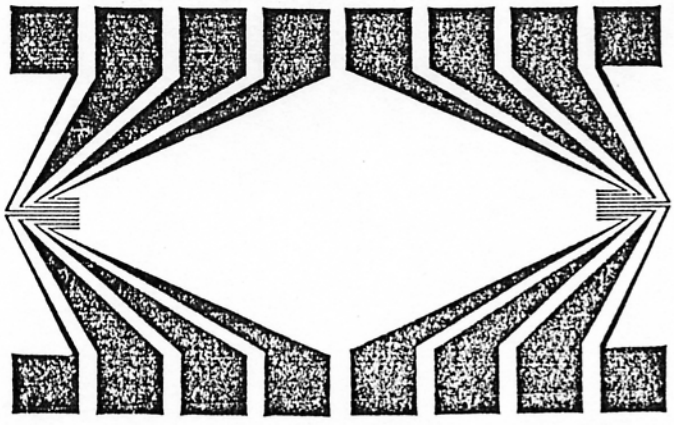

(c)

Fig.1 Mask patterns of the eight channel signal processing and computing device; (a).Channel Pattern, (b).Electrode Pattern, and (c).Lay Out From electrodes To Bonding Pads

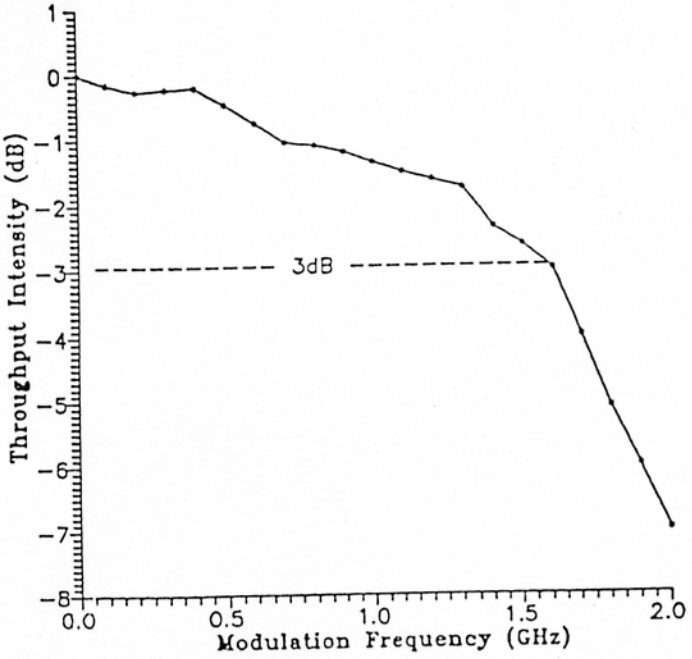

Fig.2 Bandwidth Measurement Of The Parallel 8-Bit Data Processing And Signal Modulation Device

same signs of the two bias voltages on the two corresponding electrode pads of the same channel waveguide introduce subtraction and the different signs of voltages result in addition. This high packing density cut off modulator array can do mathematical operation in parallel with 8-bit data operation simultaneously. The performance of each channel was tested separately. Fig.4 shows the results of adding two numbers. Fig.5 illustrates the results of subtracting two numbers. It is to be noted that the DC part of the throughput light was filtered out in the detection.

By integrating a laser diode array and a detector array at the two polished end faces of the modulator array, we can do parallel 8-bit addition and subtraction operation and signal processing. The relationship between bit rate per second, Br, in digital signal processing and the bandwidth of analog signal is[8]

$$Br = 2 \cdot \Omega \cdot \log_2(n) \qquad (2)$$

where n denotes the number of code levels and Ω the modulation bandwidth. In the case of binary signals, we have n=2; and the information flow, defined as the information content per second, is $2 \cdot \Omega$. The 3 db analog bandwidth of the 8 bit parallel processing array is 1.6 GHz; therefore, we have 3.2 Gbit per second binary data flow rate. This is much faster than any digital electronic computer known today. Having the benefits of high packing density and ease of fabrication, we will be able to produce much cheaper building blocks to fulfill the optical computing and multi-channel, wide-band optical signal processing on the same device configuration. All the arithmetic operations such as multiplication and dividing can be made through the combination of addition and subtraction[9].

3.2 OPTICAL NOT, OR, AND, AND NAND GATES

The typical transfer curve of the cutoff modulator is shown in Fig.6[1,2,3,7]. We define the left top region as the saturation region and the right bottom region the cutoff region. The formation of saturation region is caused by the fact that energy has to be conserved. Accordingly, there is a maximum throughput above which the drive voltage can not increase the intensity. The existence of the cutoff region is induced by the reduction of the effective index of the guided mode through external bias voltage. The shape of the transfer curve can be altered through different combinations of proton exchange condition and heat treatment. When the waveguide is biased at the cutoff region, even if a higher voltage is applied, we can not change the throughput intensity. This exclusive characteristic of the transfer curve is employed to build various kinds of optical gates through biasing the device at different points of the transfer curve and applying proper gate input signals[10]. The basic device structure is shown in Fig.7. Optical gate input signals, A and/or B, and the bias signal are added through the electrodes as indicated. We define the 0 Volt as input gate signal 0, and 5 Volts or more, depending upon the cutoff voltage of the device, to be the input gate signal 1. NOT, OR, AND, and NAND gates are realized by different combinations of bias voltages and gate signals. Optical throughput intensity is regarded as the output of the optical gate in all the gate operations.

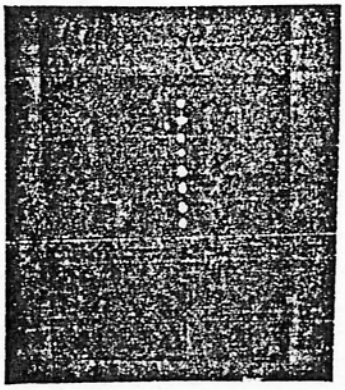

Fig.3 Near Field Image Of The Parallel 8-Bit Modulator Array

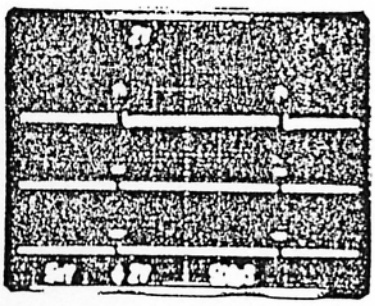

(a)

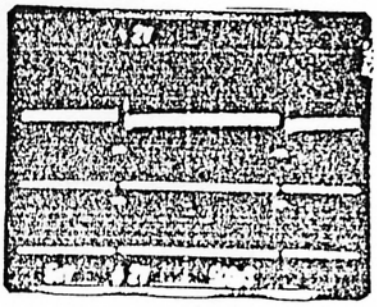

(b)

Fig.4 Results of Adding two Numbers Using one Channel of the parallel 8-Bit Modulator Array (a). 1+1=2, (b). 2+3=5

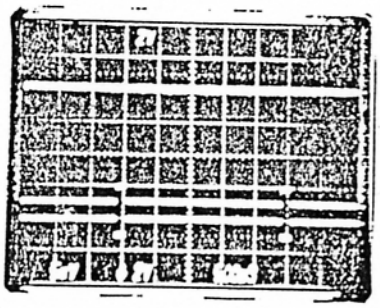

(a)

(b)

Fig.5 Results of Substracting two Numbers Using one Channel of the Parallel 8-Bit Modulator Array, (a). 1-1=0, (b). 1-4=-3

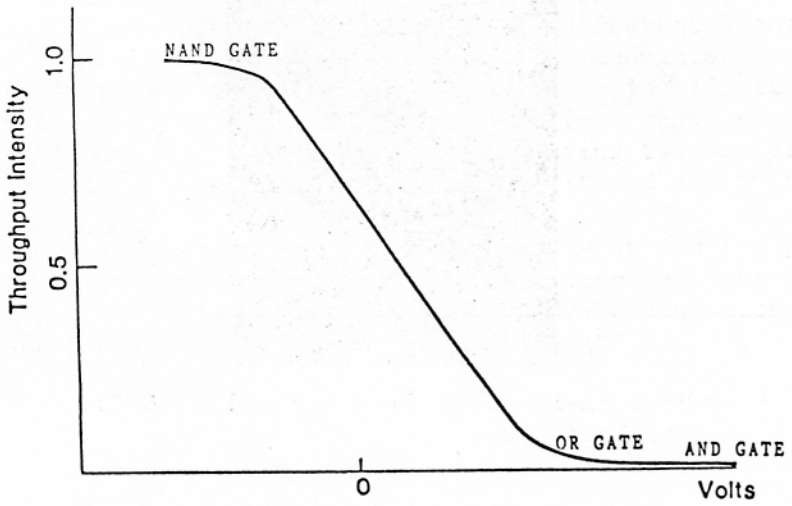

Fig.6 Typical Transfer Curve of Mode Annihilation Modulator

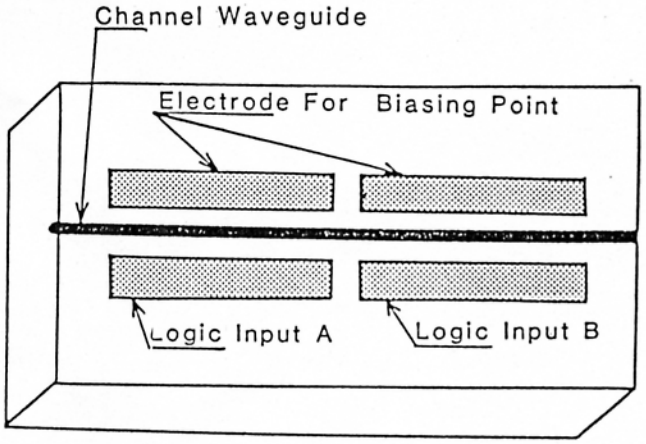

Fig.7. Device Structure of Single Channel Device for Optical Logic Gate Operation

NOT gate was easily realized using the cutoff voltage V_c=10 Volts as the input binary signal 1, and 0 Volt the input binary signal 0. The result is revealed in Fig.8. Without the application of an external voltage, namely, input was 0 state, we had the optical throughput intensity as 1. When external voltage was added to the electrode, i.e. input signal was equal to 1, the device was driven to the cutoff region with zero throughput intensity and we thus had 0 state .

The OR gate was attained with the device biased at the just cutoff region. When A and/or B was 1 (5 Volts), we shifted the operation point of the transfer curve from cutoff to the middle region. Therefore, we had the throughput intensity as output state 1. Since the device was biased at the cutoff condition, the throughput kept at the 0 state when there was no external voltage applied (A=B=0). The result is demonstrated in Fig.9. Note that the optical throughput intensity under the condition A=1, B=0 (or A=0, B=1), is different from that of A=B=1. This situation could be manipulated by using a detector with preset saturation level such that the output state 1 will be consistently observed.

In the case of AND gate, the device was biased at well below cutoff region such that, even A=1 or B=1 the operating point still stayed at the cutoff condition. The only condition when the throughput intensity was in the 1 state was when both A and B were The device operation point was shifted to the center region of the transfer curve when A=B=1. We thus could receive the optical throughput energy from the output end face of the waveguide which was regarded as the output state 1. Finally, the optical NAND gate was carried out by biasing the device at the saturation region. The throughput intensity was shifted to the center region of the transfer curve when or B is 1. The only condition that gives Y=0 was when A=B=1. Input signals A and for NAND gate operation were added from the reverse direction as that of the OR te. In this circumstance, the device is driven to the cutoff region; therefore, 0.

e ways that the gate signals A and B were added to the two parallel electrodes of ch channel waveguide depended upon the type of gate operation desired. This is due the different polarity of the electric field which changes the result of linear ectrooptic effect (Eq.(1)). The input gate signals A and B were added from the ne side of the electrode pads for NOT and NAND gates while for OR and AND gates, e A and B signals were applied reversely. The DC bias point for different gate erations are manifested in Fig.6.

4. SUMMARY

report here the formation, characterization and theory of operation of single-nnel proton-exchanged channel waveguide mode annihilation switching array. The irable effects of thermal annealing on device performance, such as the enlargement linearity, and the increase of threshold of optical damage, decrease of the drive tage and the stability of mode index, are clearly demonstrated. The theoretical culation shows that the increase of linearity is due to the proper combination of pling efficiency and electric field induced loss effect after heat treatment. table affiliation of proton exchange process, annealing status and the coupling dition will be able to give us a transfer curve with enlarged linear dynamic range ch is important for analog signal modulation.

ther applications based upon this type of device are also described. We present the first time a high packing density cutoff modulator array with wide bandwidth

and parallel signal processing capabilities. The applications of the thermally annealed single-mode channel waveguide cutoff modulator are described. Due to the exclusive characteristics, such as simplicity in design and fabrication, large linear dynamic range, and the uniqueness of the shape of the transfer curve, we can build low cost, multi-purpose electrooptic devices for optical high bit rate optical communication, optical gate operations and computing systems.

Helpful discussions and support from Dr. C. S. Tsai of UCI is acknowledged.

5. REFERENCES

1. A. Neyer and W. Sohler, " High Speed Cut-off Modulator Using A Ti-Diffused $LiNbO_3$ Channel Waveguide," Appl. Phys. Lett., Vol.35, 256 (1979)
2. P. R. Ashley and W. S. C. Chang, "Improved Mode Extinction Modulator Using Weakly Guided Channel Waveguide," Appl. Phys. Lett., Vol.45, 840(1984).
3. Ray T. Chen and C. S. Tsai, "Thermally Annealed Single-Mode Proton-Exchanged Channel Waveguide Cutoff Modulator," Optics Letters, Vol.11, 546(1986).
4. C. Baumert, C. Walter, P. Buchmann, H. Haufmann, H. Mekhior, and P. Gunter, "KNbO3 Electrooptically Induced Optical Waveguide/Cutoff Modulator," Appl. Phys. Lett., Vol.46, 1018(1985).
5. D. Hall, A. Yariv, and E. Garmire, "Observation of Propagation Cutoff and Its Control in The Thin Optical Waveguide," Appl. Phys. Lett., Vol.17, 127(1970).
6. C. Campbell, F. A. Blum, and D. W. Shaw, "GaAs Electro-Optic Channel-Waveguide Modulator," Appl. Phys. Lett., Vol.26, 640(1975)
7. R. Chen and C. S. Tsai, "GaAs-GaAlAs Heterostructure Single-Mode Channel Waveguide Cutoff Modulator and Modulator Array," Special Issue on Electrooptic Materials and Devices, IEEE J. Quantum Electron., Vol.QE-23, 2205(1987).
8. B. G. Bosch, "Gigabit Electronics A Review," Proc. IEEE, Vol.67, 340(1979).
9. A. Sawchuk and T. C. Strand, "Digital Optical Computing," IEEE Proc., Vol.72, 758(1984).
10. P. R. Ashley and W. S. C. Chang, "A Planar Waveguide Analysis of the Mode Extinction Modulator in LiNbO3," IEEE J. Quantum Electron., Vol.QE-22, 920(1986).
11. H. F. Taylor, "Guided Wave Electrooptic Devices for Logic and Computation," Appl. Opt., Vol.17, 1493(1978).

Table 1 **Design Parameters And Fabrication Conditions Of Proton-Exchanged Parallel 8 Channel Cutoff Modulator Array For Signal Processing And Computing**

PE Solution	Pure Benzoic Acid
PE Temperature	245°C
PE Time	21 Minutes
Channel Width	5 μm
Channel Length	4 mm
Channel Separation	30 μm
No. Of Channels	8
Packing Density	330/cm
Electrode Material	Cr/Al
Electrode Thickness	300/2900 Å
Electrode Width	10 μm
Measured Capacitance	3.9 pF
Electrode Length	4 mm
Measured Bandwidth	1.6 GHz

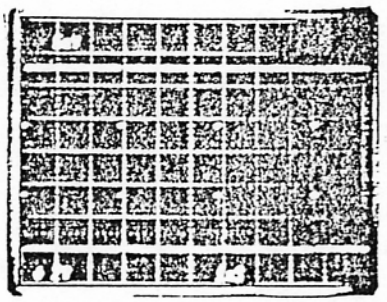

Fig.8 Optical Not Gate

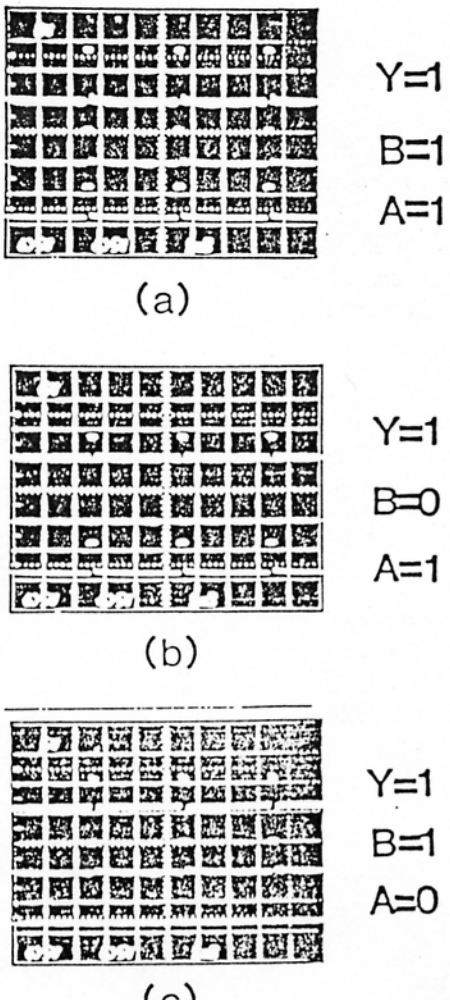

Fig.9 Optical Or Gate